

# Magnetic properties of the microorganism *Candidatus Magnetoglobus multicellularis*

Marcelo Perantoni · Darci M. S. Esquivel ·  
Eliane Wajnberg · Daniel Acosta-Avalos ·  
Geraldo Cernicchiaro · Henrique Lins de Barros

Received: 11 September 2008 / Revised: 2 February 2009 / Accepted: 18 February 2009  
© Springer-Verlag 2009

**Abstract** Magnetotactic microorganisms use the interaction of internal biomineralized nanoparticles with the geomagnetic field to orientate. The movement of the magnetotactic multicellular prokaryote *Candidatus Magnetoglobus multicellularis* under an applied magnetic field was observed. A method using digital image processing techniques was used to track the organism trajectory to simultaneously obtain its body radius, velocity, U-turn diameter, and the reorientation time. The magnetic moment was calculated using a self-consistent method. The distribution of magnetic moments and radii present two well-characterized peaks at  $(9 \pm 2) \times 10^{-15}$  and  $(20 \pm 3) \times 10^{-15} \text{ A m}^2$  and  $(3.6 \pm 0.1)$  and  $(4.3 \pm 0.1) \mu\text{m}$ , respectively. For the first time, simultaneous determination of the distribution of the organism radii and magnetic moment was obtained from the U-turn method by a new digital imaging processing. The bimodal distributions support an organism reproduction process model based on electron microscopy observations. These results corroborate the prokaryote multicellular hypothesis for *Candidatus M. multicellularis*.

**Keywords** Magnetotactic multicellular prokaryote ·  
Magnetic moment · Nanomagnetism ·  
Uncultured microorganism · U-turn method

D. M. S. Esquivel · E. Wajnberg · D. Acosta-Avalos ·  
G. Cernicchiaro · H. Lins de Barros (✉)  
Centro Brasileiro de Pesquisas Físicas,  
Rua Xavier Sigaud 150, Urca,  
22290-180 Rio de Janeiro, RJ, Brazil  
e-mail: hlins@cbpf.br

*Present address:*

M. Perantoni  
Escola de Engenharia, Universidade Federal do Rio de Janeiro,  
Cidade Universitária Bloco H, Sala H-220, Ilha do Fundão,  
21941-972 Rio de Janeiro, RJ, Brazil

## Introduction

The most important and striking feature of magnetotactic microorganisms is their response to an applied magnetic field. The large diversity of observed magnetotactic bacteria and the first described multicellular prokaryote, *Candidatus Magnetoglobus multicellularis* (GenBank EF014726) (Abreu et al. 2007), possess chains or planar arrays of biomineralized magnetic nanocrystals. These crystals impose a cell net magnetic moment which interacts with the geomagnetic field and causes the whole organism to orient along the magnetic field lines. This magnetic orientation process is a passive mechanism that depends only on this physical interaction. Direct measurement of the magnetic moment of an individual microorganism is difficult. The difficulty is associated with the low magnitude of the magnetic moment (below  $10^{-10} \text{ A m}^2$ ). The U-turn method, usually employed to estimate the total magnetic moment of magnetotactic microorganisms, is based on the study of the organism trajectory when the applied magnetic field is suddenly reversed (Lins de Barros and Esquivel 1985). On a microscopic scale, in a very low Reynolds number regime, the microorganism movement presents no inertial effects and the force is directly proportional to the velocity (Nogueira and Lins de Barros 1995). The U-turn method, however, is inaccurate due to uncertainties in measuring the trajectory diameter. Trajectories are three-dimensional, but in an optical microscope, they are restricted to the focal plane. The use of the U-turn method needs careful analyses (van Kampen 1995). An alternative method is the rotating field method (Hanzlik et al. 2002; Erghis et al. 2007). However, the U-turn method can be improved if we adopt a self-consistent criterion, as described below.

The theory of the U-turn method yields the expressions for the reorientation time ( $\tau$ ) and the diameter of the U-turn

( $L$ ) as a function of the total magnetic moment ( $\mu$ ).  $\tau$  can be measured directly by optical video microscopy observations through the number of frames recorded. Self-consistency is reached when the calculated reorientation time,  $\tau_{\text{calc}}$ , is in good agreement with the directly measured time,  $\tau_{\text{exp}}$ . This criterion strongly limits the number of useful measurements, but, on the other hand, it allows a more accurate estimate of  $\mu$ . To achieve a reliable result, it is necessary to simultaneously obtain  $\tau_{\text{exp}}$ ,  $L$ ,  $R$  (body radii),  $v$  (the migration velocity), and  $H$  (the applied magnetic field intensity).

*Candidatus M. multicellularis* was first observed in 1983 (Farina et al. 1983), and since then, it received different designations [multicellular magnetotactic aggregate, MMA (Farina et al. 1983; Farina et al. 1990), many-celled magnetotactic prokaryote, MMP (Rodgers et al. 1990), magnetotactic multicellular organism, MMO (Keim et al. 2004a, b)]. Its peculiar magnetic properties and motility, associated with biological evidences (Lins de Barros and Esquivel 1985; Keim et al. 2006; Keim et al. 2004a; Farina et al. 1983; Farina et al. 1990; Mann et al. 1990; Rodgers et al. 1990) and the phylogenetic 16 S rRNA gene sequence analysis are strong evidences that *Candidatus M. multicellularis* is a multicellular prokaryote organism with an unusual life cycle (Abreu et al. 2007; Keim et al. 2006).

*Candidatus M. multicellularis* is a spherical organism with ten to 40 gram-negative identical cells distributed in a roughly helicoidal arrangement with diameter between 6 and 9  $\mu\text{m}$ . It has a clear magnetic response and it is an example of magnetotactic microorganism. Short flagella (length 0.9 to 3.8  $\mu\text{m}$ ; Keim et al. 2006) were observed, uniformly distributed on the whole surface organism. In the cytoplasm of each cell were observed specialized organelles, magnetosomes, responsible for the biomineralization of greigite ( $\text{Fe}_3\text{S}_4$ ), a magnetic iron sulfur compound. About 60 to 100 magnetic nanocrystals of greigite were found in each constituent cell. Each crystal is enveloped by a pleomorphic magnetosome. Flow cytometry showed two size populations in the analyzed samples (Abreu et al. 2007).

*Candidatus M. multicellularis* is a magnetotactic organism, and for an efficient magnetotactic response during its life cycle, it is essential that the organism duplicates its total magnetic moment as it duplicates its volume by the growth of volume of each cell, since no unicellular phase is observed in its life cycle.

In this paper, a new method is applied to quantitatively characterize the magnetic response of *Candidatus M. multicellularis* in applied magnetic fields. This method allows the simultaneous acquisition of the U-turn method relevant physical parameters by digital imaging processing.

## Materials and methods

*Candidatus M. multicellularis* was collected in the Arauama Lagoon (22°50' S × 42°13' W), a hypersaline coastal lagoon of Rio de Janeiro state, Brazil. Water and sediment were collected at about 1 m depth, in bottles of 500 mL and kept in the laboratory in an aquarium of 12 × 14 × 20 cm (width × height × length) for several months. The aquarium was kept under a high degree of insolation and the salinity was maintained similar to the original level (~60‰) by addition of fresh water. A magnet was used to concentrate the sample in a special glass container (Lins de Barros et al. 2004). After a few minutes, the organisms were collected in the capillary extremity of the glass container with a pipette and transferred to a microscope slide.

A standard digital camera (Sony Digital 8 DCR-TRV 110-NTSC), optically adapted to an optical microscope (Zeiss-JenaVal, objectives ×10 and ×25), recorded the organism movement. The camera frame rate was 30 fps. A pair of coils (3.5 cm diameter, 4.4 cm gap) was adapted to the microscope. A DC current power supply, controlled by a microcomputer, generated a square wave magnetic field (about 2–15 G magnitude and frequency range from 0.1 to 1.2 Hz) synchronized with the image recording. The pixel to length (in micrometers) ratio was calibrated with a micrometer grid. The videos were transferred from the camera to the microcomputer via a standard firewire interface. In order to reduce noise and to prepare images for further processing, an appropriate sequence of algorithms and standard digital filters were applied. A vector (position  $x$ ,  $y$ , and  $R$ ) was associated to each organism in each frame. To follow the organism frame-by-frame, a circumference with radius previously chosen and centered in the center of the organism was generated. Each image was compared to the one from the next frame. If an organism is found inside the circumference defined in the previous frame, it is identified as the same organism, receiving a common label in both images (Fig. 1A, circles a, b, and c). If, however, more than one organism are found within the circumference (Fig. 1A, circle d) or one organism within two or more circumferences (Fig. 1A, circle e), the data is discarded. This procedure was repeated for all frames determining the organism trajectory as shown in Fig. 1B.

As we are interested in measuring magnetic properties, the use of laboratory fields much higher than the local geomagnetic field (in Rio de Janeiro ~0.25 Oe) is the best choice to minimize the contribution of biological effects such as flagellar action. The use of a square wave field with period greater than the U-turn time allows us to obtain several U-turn trajectories of

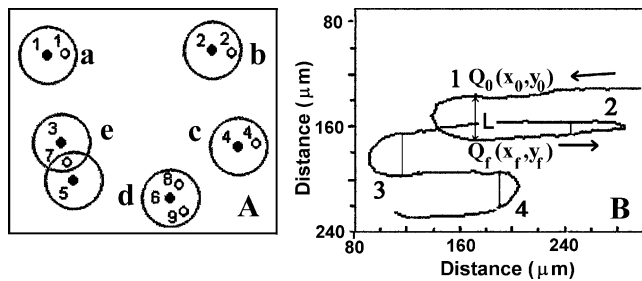


**Fig. 1** **A** Representative scheme of organism labeling and trajectories determination. *Small full circles* correspond to organisms in frame *N*. *Small open circles* correspond to organisms in frame *N+1*. *a, b, and c* are prefixed circumferences where organisms 1, 2, and 4 are identified, respectively, while in *d* and *e* circumferences organisms 3, 5–9 are discarded. **B** Trajectory of one organism observed during 4.2 s. Four U-turns are noted. The magnetic field (1.3 Oe and 1.2 Hz) is parallel to the horizontal axis.  $Q_0$  is the position where the field was suddenly reversed and  $Q_f$  is the end point of the U-turn.  $L$  is the U-turn diameter.  $Q_0$ ,  $Q_f$ , and  $L$  are indicated for U-turn 1. U-turn 2 was discarded by the self-consistent criterion

the same organism. *Candidatus M. multicellularis* is an anaerobic organism and its observed behavior in the present work can be affected by the presence of molecular oxygen. However, we do not expect any change of its magnetic properties, the aim of the present work. The observed trajectories are then different of those in natural habitat conditions (0.25 Oe field, low  $O_2$  concentration). The magnetic properties, which are the aim of the present work, do not change.

Figure 1B shows an example of a trajectory obtained by this digital procedure. The U-turn diameter,  $L$ , and the migration velocity,  $v$ , were simultaneously obtained from the vectors associated with the trajectory. The experimental U-turn time,  $\tau_{exp}$ , was determined counting the number of frames between  $Q_0$ , the position where the field was suddenly reversed, and  $Q_f$ , the end point of the U-turn. The body radius,  $R$ , was estimated from the number of pixels in the digitalized image.

The magnetic moment  $\mu$  is then calculated based on the U-turn equation (Esquivel and Lins de Barros 1986; Keim et al. 2006):

$$\mu = 8\pi^2 \eta R^3 v / (LH) \tag{1}$$

where  $\eta$  is the water viscosity ( $10^{-2}$  poise) and  $v$  is the migration velocity of the organism.  $\tau_{calc}$  is given by:

$$\tau_{calc} = [8\pi \eta R^3 / (\mu H)] \ln [2\mu H / (k_B T)] \tag{2}$$

where  $k_B$  is the Boltzmann constant and  $T$  is the room temperature (300 K).

Measurements with the difference (estimated error) between  $\tau_{exp}$  and  $\tau_{calc}$  greater than 20% were discarded. With this criterion, about 60% of the measurements were discarded. This self-consistent criterion permits to discard  $L$  values obtained from images corresponding to trajectories in a plane not parallel to the focal plane, which would result in false  $\mu$  values.

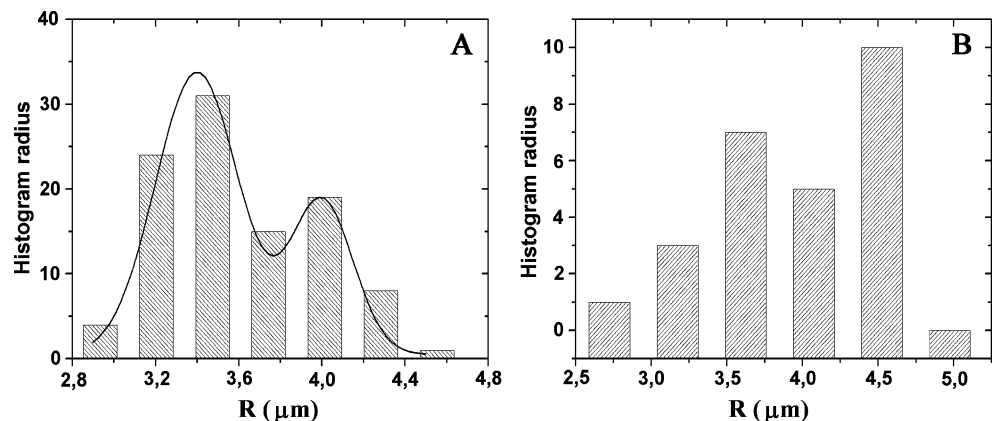
Scanning electron microscopy (SEM) samples were fixed with 2.5% glutaraldehyde in 0.1 sodium cacodylate buffer, washed with fresh water, dehydrated in acetone series, gold sputtered, and observed in a SEM JEOL JSM 5800 at 20 kV.

**Results**

All the organisms analyzed were south seeking. This means they swim in the direction of the north magnetic pole. It was observed by the video microscopy that *Candidatus M. multicellularis* swims in a very elongated helical trajectory with velocities in the range of 50 to 150  $\mu\text{m/s}$ , depending on the sample condition.

The radii of 110 *Candidatus M. multicellularis* were measured from SEM micrograph and their distribution is shown in the histogram of Fig. 2A. Sturges' rule was used to determine the number of bins. The curve in this figure is

**Fig. 2** Histogram of the *Candidatus M. multicellularis* radius,  $R$ . **A** Radii obtained by SEM. Line is the best fit with two Gaussian curves centered at  $(3.4 \pm 0.1)$  and  $(4.0 \pm 0.1) \mu\text{m}$ . Note that these organisms seem to be smaller than those observed by optical microscopy; however, this can be due to the fixation process. **B** Radii of 60 organisms obtained using the video images and digital filter method. Two peaks are observed at  $(3.6 \pm 0.1)$  and  $(4.3 \pm 0.1) \mu\text{m}$



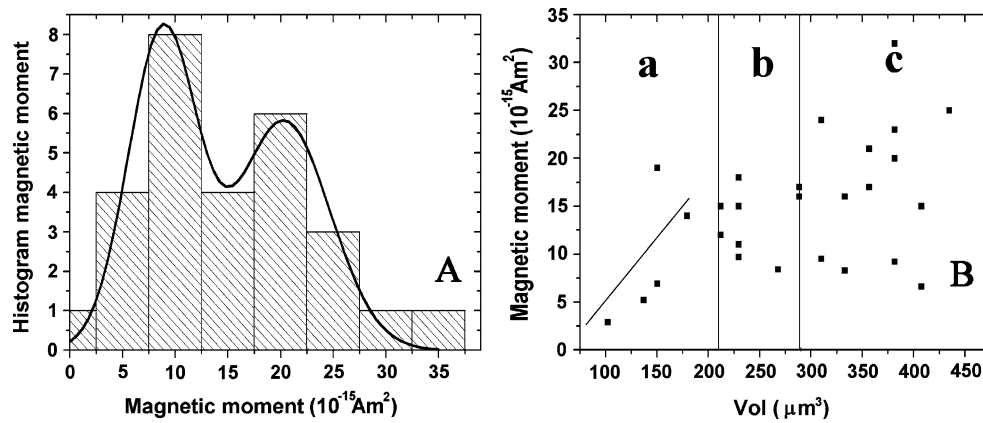


**Fig. 3** **A** Histogram of 28 *Candidatus M. multicellularis* magnetic moments,  $\mu$ . Line is the best fit with two Gaussian curves. Two peaks at  $(9 \pm 2)$  and  $(20 \pm 3) \text{A m}^2$  are clearly observed. The self-consistent criterion was used. **B** Organism magnetic moment,  $\mu$ , plotted against volume, Vol. Three regions are observed. In *a* ( $\text{Vol} < 210 \mu\text{m}^3$ ;  $R <$

$3.7 \mu\text{m}$ ), a linear correlation is observed (correlation coefficient 0.68). In *b* ( $210 \mu\text{m}^3 < \text{Vol} < 290 \mu\text{m}^3$ ;  $3.7 \mu\text{m} < R < 4.1 \mu\text{m}$ ),  $\mu$  falls in a narrow value range. In region *c* ( $\text{Vol} > 290 \mu\text{m}^3$ ;  $R > 4.12 \mu\text{m}$ ), a large dispersion of values of  $\mu$  is observed, but the largest values of  $\mu$  are in this region

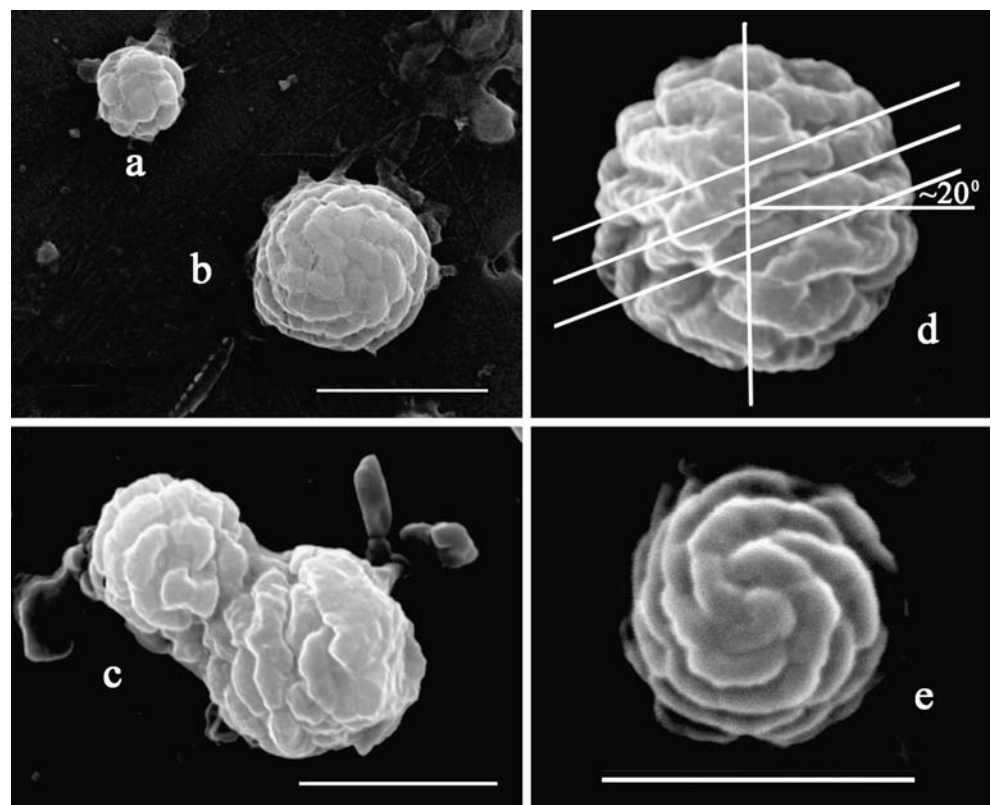
the best fit using two Gaussian curves with peaks at  $(3.4 \pm 0.1)$  and  $(4.0 \pm 0.1) \mu\text{m}$ . Using video images with digital filter method, the distribution of 60 microorganism radii was obtained and also shows two peaks, centered in  $(3.6 \pm 0.1)$  and  $(4.3 \pm 0.1) \mu\text{m}$  (Fig. 2B).

The distribution of the magnetic moments,  $\mu$ , of 28 *Candidatus M. multicellularis* selected by the self-consistency criterion also presents two peaks (Fig. 3A). It

was fitted with two Gaussian curves with peaks at  $(9 \pm 2) \times 10^{-15}$  and  $(20 \pm 3) \times 10^{-15} \text{A m}^2$ . Figure 3B shows the magnetic moment as a function of the volume of these 28 organisms. Although there is no direct correlation, we observe that the greatest values of  $\mu$  are in the region of larger volume.

Figure 2 shows two size populations that are in agreement with its life cycle proposed for this organism

**Fig. 4** SEM images **a–c** illustrate three phases of the life cycle of *Candidatus M. multicellularis* (bar =  $5 \mu\text{m}$ ). **a** Phase 1. The organism has a small volume. **b** The organism has grown and each cell divided synchronously. **c** The organism changes its spherical shape, constricting the middle region. These micrographs were obtained using samples collected in different days than those used in the optical microscopy, but in the same place. Bar =  $5 \mu\text{m}$ . **d** and **e** Two *C. magnetoglobus multicellularis* showing that it is spherical multicellular organism and composed of cells distributed in a spiral array. **d** A side view of an organism showing the orientation of cells with respect to the equatorial plane ( $20^\circ$ ). **e** A top view of one organism. The complex helicoidal distribution of cells is clearly observed. Bar =  $5 \mu\text{m}$





(Abreu et al. 2007; Keim et al. 2006). The ratios between the two peaks [3.4 and 4.0  $\mu\text{m}$  in Fig. 2A (ratio=1.18) and 3.6 and 4.3  $\mu\text{m}$  in Fig. 2B (ratio=1.19)] are in good agreement with the value expected to double the volume ( $2^{1/3}=1.26$ ).

Coherently, the relation between the two values of  $\mu$  in Fig. 3A is 2.2 and is consistent with the existence of doubled volume and doubled total magnetic moment such that an effective magnetic response is guaranteed. Figure 3B shows the relation between  $\mu$  and the total volume, Vol, of 28 organisms.

## Discussion

The samples were collected directly from their natural habitat, maintained in laboratory in an aquarium. Since *Candidatus M. multicellularis* are flagellated organisms, samples collected after magnetic concentration procedure is a representative statistical sample of the population. It is observed (Keim et al. 2004a, b, 2006) that these organisms are composed by cells closely apposed and organized in a characteristic way. The magnetic properties of this organism reflects and, in some way, are directly associated to its life cycle.

Reported observations (Abreu et al. 2007) suggest that, during the life cycle, each cell component grows, doubling the volume of the whole organism and its magnetic moment. After this growing, a synchronous division of all the cells is observed. In the following phase, the organism elongates and constricts at the middle, giving rise to two new equivalent organisms (Fig. 4a–c).

Based on the observations of this paper, it is suggested that the life cycle of *Candidatus M. multicellularis* has five phases. In the first phase, the organism has a mean radius of about 3.6  $\mu\text{m}$  (Figs. 2b and 4a) and a total magnetic moment of the order of  $9 \times 10^{-15} \text{ A m}^2$  (Fig. 3A). During this phase, the component cells grow in volume and produce nanocrystals. As shown in Fig. 3B (region a), small organisms ( $\text{Vol} < 210 \mu\text{m}^3$ ,  $R < 3.7 \mu\text{m}$ ) present a linear correlation between the magnetic moment and the volume (correlation coefficient 0.68).

The second phase of its life cycle is characterized by a rapid growth in volume (Fig. 4b) and a low rate of crystal production. The magnetic moment value falls in a narrow range. This phase can be associated to the volume range ( $210 \mu\text{m}^3 < \text{Vol} < 290 \mu\text{m}^3$ ,  $3.7 \mu\text{m} < R < 4.1 \mu\text{m}$ ) shown in region b of Fig. 3B.

The third phase is similar to the first one. In this phase, the organism has a large volume ( $\text{Vol} > 290 \mu\text{m}^3$ ,  $R > 4.1 \mu\text{m}$ ) and it continues to produce magnetic material (Fig. 3B, region c).

The fourth phase is characterized by the synchronous division of constituent cells. In this phase, it is possible that the organism reorganizes the cells. If this actually happens, it is possible that the total magnetic moment changes because of changes in the vectorial sum of the magnetic moment of each cell. Figure 3B shows a large dispersion of  $\mu$  in the region of volume higher than  $290 \mu\text{m}^3$ . This phase is also related to the data in region c of Fig. 3B.

The last phase is the process of constriction and division itself (Fig. 4c). It was not observed by optical microscopy and that only considered spherical individuals in the digital process. Substantial production of biomineralized magnetic crystals is not probable to occur in the last phase, but certainly a rearrangement of the internal distribution of crystals should occur (Fig. 4a–c).

The whole organism contains about 600 to 4,000 crystals, arranged in a helical distribution. These crystals are parallelepiped-shaped biomineralized magnetic greigite crystals (0.88  $\mu\text{m}$  length; 0.71  $\mu\text{m}$  width, and average volume  $V_{\text{crystal}} = 0.44 \mu\text{m}^3$ ) and are located in the magnetosomes. The magnetosomes are arranged in planar groups, with the magnetic moment of individual cells probably tangent to the helix and forming an angle of less than  $20^\circ$  with the equatorial plane (Fig. 4d, e). The maximum expected magnetic moment in this simplified model is given by:

$$\mu_{\text{max}} = N \times M_g \times m_{\text{greigite}} \times \sin 20^\circ \quad (3)$$

where  $N$  is the number of magnetic crystals (600–4,000),  $M_g$  is the mass of one greigite crystal ( $4.1 \times 10^{-15} \text{ g}$ ) and  $m_{\text{greigite}}$  is the saturation magnetization of greigite [several values are reported in the literature, being in the range ( $14$ – $59 \times 10^{-3} \text{ A m}^2/\text{g}$ )] (Dekkers and Schoonen 1996; Chang et al. 2008).  $\mu_{\text{max}}$  is then in the range  $(1.2$ – $7.8) \times 10^{-14} \text{ A m}^2$ .

As the degree of magnetic optimization of *Candidatus M. multicellularis* is 80% at most (Winklhofer et al. 2007), the maximum expected magnetic moment of the organism,  $\mu_{\text{expected}}$ , is in the range  $(10$ – $75) \times 10^{-15} \text{ A m}^2$  and the  $\mu$  values obtained in this paper are in the expected region of an optimized magnetotactic organism.

In conclusion, a new digital process was used with the traditional optical microscopy set-up for magnetotactic organisms U-turn analysis. The system was successfully tested to simultaneously obtain the U-turn trajectory parameters, which are necessary to calculate the magnetotactic organism magnetic moment. Individual magnetic moments of the order of  $10^{-15} \text{ A m}^2$  were estimated, a value much lower than the sensitivity limit of SQUID magnetometers, without requiring concentrated *Candidatus M. multicellularis* samples. With the results obtained from this new method, new characteristics about the life cycle of *Candidatus M. multicellularis* were suggested.

**Acknowledgements** M. Perantoni thanks the Ministério da Ciência e Tecnologia for a fellowship. We thank Major André Pinto from the Instituto Militar de Engenharia (IME) for the use of the SEM facilities and Dr. Diana Guenzburger for the English revision.

## References

- Abreu F, Martins JL, Silveira TS, Keim CN, Lins de Barros HGP, Gueiros Filho FJ, Lins U (2007) '*Candidatus Magnetoglobus multicellularis*', a multicellular, magnetotactic prokaryote from a hypersaline environment. *IJSEM* 57:1318–1322
- Chang L, Roberts AP, Tang Y, Rainford BD, Muxworthy AR, Chen QW (2008) Fundamental magnetic parameters from pure synthetic greigite ( $\text{Fe}_3\text{S}_4$ ). *J Geophys Res* 113:B06104
- Dekkers MJ, Schoonen MAA (1996) Magnetic properties of hydrothermally synthesized greigite ( $\text{Fe}_3\text{S}_4$ )—I. Rock magnetic parameters at room temperature. *Geophys J Int* 126:360–368
- Erghis K, Wen Q, Ose V, Zeltins A, Shapiro A, Janney PA, Cēbers A (2007) Dynamics of magnetotactic bacteria in a rotating field. *Biophys J* 93:1402–1412
- Esquivel DMS, Lins de Barros H (1986) Motion of magnetotactic microorganisms. *J Exp Biol* 121:153–163
- Farina M, Lins de Barros HGP, Esquivel DMS, Danon J (1983) Ultrastructure of a magnetotactic microorganism. *Biol Cell* 48:85–88
- Farina M, Esquivel DMS, Lins de Barros HGP (1990) Magnetic iron-sulphur crystals from a magnetotactic microorganism. *Nature* 343:256–258
- Hanzlik M, Winklhofer M, Petersen N (2002) Pulsed-field remanence measurements on individual magnetotactic bacteria. *J Magn Magn Mater* 248:258–267
- Keim CN, Abreu F, Lins U, Lins de Barros HGP, Farina M (2004a) Cell organization and ultra structure of a magnetotactic multicellular organisms. *J Struct Biol* 145:254–262
- Keim CN, Martins JL, Abreu F, Rosado AS, Lins de Barros HGP, Borojevic R, Lins U, Farina M (2004b) Multicellular life cycle of magnetotactic prokaryotes. *FEMS Microbiol Lett* 240:203–208
- Keim CN, Martins JL, Lins de Barros H, Lins U, Farina M (2006) Structure, behavior, ecology and diversity of multicellular magnetotactic prokaryotes. In: Schüler D (ed) *Magnetoreception and magnetosomes in bacteria*. Springer, Berlin, pp 103–132
- Lins de Barros HGP, Esquivel DMS (1985) Magnetotactic microorganisms found in muds from Rio de Janeiro. In: Kirschvink JL, Jones DS, MacFadden BJ (eds) *Magnetite biomineralization and magnetoreception in organisms*. Plenum Press, New York, pp 289–309
- Lins de Barros HGP, Esquivel DMS, Farina M, Lins U, Keim CN (2004) Simple homemade apparatus for harvesting uncultured magnetotactic microorganism. *Braz J Microbiol* 94:111–116
- Mann S, Sparks NHC, Frankel RB, Bazylinski DA, Jannasch HW (1990) Biomineralization of ferrimagnetic greigite ( $\text{Fe}_3\text{S}_4$ ) and iron pyrite ( $\text{FeS}$ ) in a magnetotactic bacterium. *Nature* 343:258–261
- Nogueira FS, Lins de Barros H (1995) Study on the motion of magnetotactic bacteria. *Eur Biophys J* 24:13–21
- Rodgers FG, Blakemore RP, Blakemore RA, Frankel RB, Bazylinski DA, Maratea D, Rodgers C (1990) Intercellular structure in a many-celled magnetotactic prokaryote. *Arch Microbiol* 154:18–22
- Van Kampen NG (1995) The turning of magnetotactic bacteria. *J Stat Phys* 80:23–33
- Winklhofer M, Abraçado LG, Davila AF, Keim CN, Lins de Barros HGP (2007) Magnetic optimization in a multicellular magnetotactic organism. *Biophys J* 92:661–670